Journal of Zhejiang University-SCIENCE C (Computers & Electronics)
ISSN 1869-1951 (Print); ISSN 1869-196X (Online)
www.zju.edu.cn/jzus; www.springerlink.com
E-mail: jzus@zju.edu.cn

Blind carrier frequency offset estimation for constant modulus signaling based OFDM systems: algorithm, identifiability, and performance analysis*

Wei-yang XU†[1], Bo LU[1], Xing-bo HU[2], Zhi-liang HONG[1]

([1]*Department of Microelectronics, Fudan University, Shanghai 201203, China*)

([2]*School of Information Science and Technology, East China Normal University, Shanghai 200241, China*)

†E-mail: weiyangxu@fudan.edu.cn

Received Mar. 14, 2009; Revision accepted June 4, 2009; Crosschecked Sept. 29, 2009

Abstract: Carrier frequency offset (CFO) estimation is critical for orthogonal frequency-division multiplexing (OFDM) based transmissions. In this paper, we present a low-complexity, blind CFO estimator for OFDM systems with constant modulus (CM) signaling. Both single-input single-output (SISO) and multiple-input multiple-output (MIMO) systems are considered. Based on the assumption that the channel keeps constant during estimation, we prove that the CFO can be estimated uniquely and exactly through minimizing the power difference of received data on the same subcarriers between two consecutive OFDM symbols; thus, the identifiability problem is assured. Inspired by the sinusoid-like cost function, curve fitting is utilized to simplify our algorithm. Performance analysis reveals that the proposed estimator is asymptotically unbiased and the mean square error (MSE) exhibits no error floor. We show that this blind scheme can also be applied to a MIMO system. Numerical simulations show that the proposed estimator provides excellent performance compared with existing blind methods.

Key words: Orthogonal frequency-division multiplexing (OFDM), Constant modulus (CM), Carrier frequency offset (CFO), Blind estimation, Multiple-input multiple-output (MIMO)

doi:10.1631/jzus.C0910150 **Document code:** A **CLC number:** TN929.5

1 Introduction

Orthogonal frequency-division multiplexing (OFDM) is more vulnerable to carrier frequency offset (CFO) than single-carrier systems (Nee and Prasad, 2000). Introduced by the Doppler shifts or the mismatch between transmit and receive oscillators, CFO can lead to intercarrier interference (ICI) and reduction in amplitude for the desired subcarriers, resulting in a severe degradation in bit error rate (BER) performance (Pollet *et al*., 1995). Therefore, CFO estimation is of great importance in OFDM systems and has received extensive attention in the literature.

Generally speaking, CFO estimators can be classified into data-aided and blind methods. Data-aided estimators, which are mainly suited for burst packet transmissions (Morelli *et al*., 2007), rely on periodically transmitted training symbols (Moose, 1994; Schmidl and Cox, 1997; Morelli *et al*., 2000; Minn *et al*., 2003; 2006) or pilots (Coulson, 2001; Yu and Su, 2004; Gao *et al*., 2008). These methods achieve high estimation accuracy at the expense of bandwidth efficiency, indicating relatively low attractiveness for continuous transmissions (Ai *et al*., 2006).

Many blind estimators have also been proposed to improve the bandwidth efficiency. The methods using the cyclic prefix (CP) preceding OFDM symbols have low complexity (Beek *et al*., 1997; Hsieh and Wei, 1999; Lashkarian and Kiaei, 2000), but their performance is not guaranteed in mobile environments since part of the CP is inevitably blurred by multipath effects. A large number of blind estimators

* Project supported by the Intel Research Council and the Applied Materials Shanghai Research & Development Fund (No. 0507)

take advantage of the null or virtual subcarriers (VSCs) existing in many OFDM systems (Liu and Tureli, 1998; Tureli *et al*., 2000; 2001; 2004; Ma *et al*., 2001; Huang and Letaief, 2006). This idea was originally introduced by Liu and Tureli (1998), where the inherent orthogonality between VSCs and information bearing subcarriers is exploited to estimate the CFO. Although highly accurate and robust to the channel multipath, this subspace-based estimator may suffer from the identifiability problem (Ma *et al*., 2001). Two techniques, exploiting distinctively spaced VSCs and randomly hopping VSCs, were proposed to solve the identifiability problem (Ma *et al*., 2001), but the complexity is relatively high since the line search method is used to minimize the cost function. Amongst other recently proposed algorithms, the diagonality criterion based method estimates the CFO via minimizing the total off-diagonal power in the signal covariance matrix, and the spectral method tracks the location of the ripple peaks to provide an estimate of CFO with the help of a comb filter (Roman *et al*., 2006; Talbot and Boroujeny, 2008). Both of them yield efficient bandwidth utilization since no pilots or VSCs are required.

Intense attention has been given over recent years to multiple-input multiple-output (MIMO) techniques, which dispose multiple antennas at both transmitter and receiver sides to provide spatial diversity and capacity gains (Stüber *et al*., 2004). Yao and Giannakis (2005) introduced a kurtosis metric based on the observation that the distribution of the received signal has the maximum non-Gaussianity when there is no CFO for the CFO estimation in MIMO-OFDM systems. Using curve fitting, this method can obtain highly accurate results with low complexity, but this is true only when the results are averaged over a large number of OFDM symbols. To minimize this process delay, Zeng and Ghrayeb (2008) proposed a constant modulus (CM) signaling based algorithm. It accomplishes the estimation procedure using only one OFDM symbol with the assumption that the channel frequency response on two neighboring subcarriers is approximately the same. However, we will show that minimizing Zeng's cost function would not render an exact estimate of the CFO and its performance degrades severely as the channel's frequency selectivity becomes more pronounced.

In this paper, we present a blind CFO estimator for both single-input single-output (SISO) OFDM and MIMO-OFDM systems with CM signaling. The proposed method does not require a priori knowledge of the transmitted data or the multipath channel. Also, no pilots or VSCs are needed so that all subcarriers can be used to transmit data although is still applicable in the presence of VSCs. The only requirement is that the channel keeps constant during estimation, which is also assumed in (Yao and Giannakis, 2005; Zeng and Ghrayeb, 2008) and most frame based transmissions, e.g., IEEE 802.11a (1999) and IEEE 802.16d (2004). Under this assumption, we find that the square amplitudes of the received data on the same subcarriers in two consecutive OFDM symbols are identical in the absence of CFO. This finding forms our cost function which measures the power difference of data on the same subcarriers between two consecutive OFDM symbols. It is shown that minimizing the cost function yields a unique and exact estimate of the CFO in the noise free case; thus, the identifiability problem is assured. We also exploit curve fitting to simplify the proposed algorithm. Furthermore, we derive the theoretical mean and the mean square error (MSE) of the proposed algorithm. It is shown that our estimator is asymptotically unbiased and the theoretical MSE fits the simulation results quite well at medium to high signal-to-noise ratio (SNR) values. With the help of Alamouti (1998)'s scheme, the proposed method is then applied in MIMO-OFDM systems. Numerical results show that our proposed method performs better than Yao's and Zeng's algorithms in both SISO and MIMO systems over different multipath channels.

Notations: Upper- and lower-case bold symbols denote the matrices and column vectors, respectively; $\boldsymbol{A}^{\mathrm{T}}$ denotes the transpose of $\boldsymbol{A}$; $\boldsymbol{A}^{\mathrm{H}}$ stands for the conjugate transpose of $\boldsymbol{A}$; $[\boldsymbol{W}]_{mn}=(N)^{-1/2}\exp(\mathrm{j}2\pi mn/N)$ is the $N\times N$ inverse discrete Fourier transform (IDFT) matrix; $\{\}^*$ refers to the elementwise conjugation. $\boldsymbol{I}_N$ indicates the identity matrix with size $N\times N$. $\mathrm{diag}\{a_1, a_2, \ldots, a_N\}$ denotes the diagonal matrix with $a_1, a_2, \ldots, a_N$ on the main diagonal. $E\{\}$ represents the expectation. $|\cdot|$ indicates the corresponding amplitude, while $\Re\{\}$ denotes the real components.

2 SISO-OFDM system model

We will refer to SISO-OFDM as OFDM for concision in the following analysis. Assuming there are N subcarriers used for the data transmission, let Eq. (1) denotes the mth data block to be transmitted:

$$\boldsymbol{d}(m)=\left[d_{m,0}, d_{m,1}, \ldots, d_{m,N-1}\right]^{\mathrm{T}}, \tag{1}$$

where $d_{m,n}$ (n=0, 1, …, N−1) is the source symbol drawn from a CM constellation with zero mean and variance σ_d^2. In typical OFDM systems, N complex data are modulated onto N mutually orthogonal subcarriers via the IDFT at the transmitter. Using matrix representation, the mth data block after modulation is

$$\boldsymbol{x}(m)=[x_{m,0}, x_{m,1}, \ldots, x_{m,N-1}]^{\mathrm{T}}=\boldsymbol{W}\boldsymbol{d}(m). \tag{2}$$

The CP, which is a copy of the last L samples of the modulated data, is prefixed to form an OFDM symbol and its length is assumed to be longer than the maximum channel delay spread to avoid intersymbol interference (ISI). The resultant baseband signal is up-converted to radio frequency (RF) and transmitted through the multipath channel. In the receiver end, there usually coexist timing offset and CFO in the down-converted received signal. We assume that the timing synchronization—devoted to finding the correct position of discrete Fourier transform (DFT) window—is perfectly achieved. Therefore, the CP is removed and the remaining N samples are fed into the DFT processor for demodulation. With a CFO normalized by the subcarrier spacing as ε, the DFT output of the mth received data block is

$$\boldsymbol{y}(m)=\mathrm{e}^{\mathrm{j}2\pi\varepsilon[(m-1)N+mL]/N}\boldsymbol{W}^{\mathrm{H}}\boldsymbol{\Phi}(\varepsilon)\boldsymbol{W}\boldsymbol{H}\boldsymbol{d}(m)+\boldsymbol{w}(m), \tag{3}$$

where $\boldsymbol{w}(m)\sim\mathrm{CN}(0, \sigma_n^2\boldsymbol{I}_N)$ represents the additive white Gaussian noise (AWGN), and $\boldsymbol{\Phi}$ and $\boldsymbol{H}$ denote the CFO matrix and channel frequency response matrix, respectively:

$$\begin{cases}\boldsymbol{\Phi}(\varepsilon)=\mathrm{diag}\left\{1, \mathrm{e}^{\mathrm{j}2\pi\varepsilon/N}, \ldots, \mathrm{e}^{\mathrm{j}2\pi(N-1)\varepsilon/N}\right\},\\ \boldsymbol{H}=\mathrm{diag}\left\{H_{m,0}, H_{m,1}, \ldots, H_{m,N-1}\right\}.\end{cases} \tag{4}$$

In this study, we suppose that the channel is slow fading so that it remains constant while the estimation is performed. The proposed algorithm is aimed at estimating the fractional CFO, i.e., $\varepsilon\in[-0.5, 0.5]$. For more general cases, our method can be combined with VSCs based algorithms to enlarge the acquisition range or we may use other means (Schmidl and Cox, 1997) to reduce the initial larger CFO. If there is no CFO, signals on the nth subcarrier of the mth received OFDM symbol would be

$$y_{m,n}=d_{m,n}H_{m,n}+w_{m,n},\quad n=0,1,\ldots,N-1. \tag{5}$$

Thus, a single-tap equalizer can be used to recover data, which is one of the merits of OFDM techniques. On the other hand, ICI will occur because of the loss of mutual orthogonality between subcarriers. Then we have

$$y_{m,n}=\mathrm{e}^{\mathrm{j}\frac{2\pi\varepsilon}{N}[(m-1)N+mL]}\left(I_0 d_{m,n}H_{m,n}+\sum_{l=0,l\neq n}^{N-1}I_{l-n}d_{m,l}H_{m,l}\right)+w_{m,n},\quad n=0,1,\ldots,N-1, \tag{6}$$

where

$$I_n=\frac{\sin(\pi\varepsilon)}{N\sin(\pi(\varepsilon+n)/N)}\exp\left(\mathrm{j}\frac{\pi}{N}\left((N-1)\varepsilon-n\right)\right). \tag{7}$$

We find that the CFO results in amplitude reduction for the desired subcarrier and a power leakage from others, and consequently causes BER degradation. Therefore, the estimation and compensation of CFO should be accomplished with high fidelity.

3 Proposed CFO estimation scheme for SISO-OFDM systems

3.1 Proposed algorithm

To counteract the detrimental effect of CFO, a compensation matrix is generally applied to the received data before DFT. Supposing that the estimated CFO is denoted by $\hat{\varepsilon}$, the mth received data block after CFO compensation and DFT is

$$\boldsymbol{y}(m)=\mathrm{e}^{\mathrm{j}2\pi\varepsilon[(m-1)N+mL]/N}\boldsymbol{W}^{\mathrm{H}}\boldsymbol{\Phi}(\varepsilon-\hat{\varepsilon})\boldsymbol{W}\boldsymbol{H}\boldsymbol{d}(m)+\boldsymbol{v}(m), \tag{8}$$

where $\boldsymbol{v}(m)$ has the same statistical property as $\boldsymbol{w}(m)$.

In the absence of noise, if there is perfect CFO compensation, the data on the nth subcarrier reduce to $d_{m,n}H_{m,n}$. Similarly, the counterpart in the (m+1)th data block is $d_{m+1,n}H_{m+1,n}$. Applying the square amplitude operation on these two terms, we have

$$\left|d_{m,n}H_{m,n}\right|^2=\left|d_{m+1,n}H_{m+1,n}\right|^2, \tag{9}$$

since the channel frequency response keeps constant over two consecutive OFDM symbol durations and the square amplitudes of signal can be simply removed from both sides when CM signaling is adopted. This observation enlightens us to formulate a cost function that searches for an estimated CFO to minimize the power difference of data on the same subcarriers between two consecutive OFDM symbols, i.e.,

$$J(\tilde{\varepsilon})=\sum_{n=0}^{N-1}\left(\left|y_{m,n}(\tilde{\varepsilon})\right|^2-\left|y_{m+1,n}(\tilde{\varepsilon})\right|^2\right)^2, \tag{10}$$

where $\tilde{\varepsilon}=\varepsilon-\hat{\varepsilon}$. Compared with Zeng's method where only one OFDM symbol is used to complete a single estimation, the proposed algorithm needs the observation of two consecutive OFDM symbols. However, it will be shown that our estimator offers an excellent performance in spite of this minor processing delay.

3.2 Identifiability problem

It is readily understood that the cost function in Eq. (10) reaches its minimum, namely 0, when CFO is correctly compensated. Then we come to the identifiability problem which involves whether minimizing the cost function yields a unique and exact estimate of the CFO. In a noise free case, our cost function can be simplified as

$$J(\tilde{\varepsilon})=A\cos(2\pi\tilde{\varepsilon})+B\sin(2\pi\tilde{\varepsilon})+C, \tag{11}$$

where A, B and C are constants which depend only on data and channel realization (for details of derivation, see Appendix A). Note that the cost function reaches 0 when $\hat{\varepsilon}=\varepsilon$, i.e.,

$$J(0)=A+C=0 \;\Rightarrow\; A=-C \text{ and } A<0. \tag{12}$$

Also, given that our cost function is nonnegative and continuous over the concerned CFO range, the first order derivative of Eq. (11) must be 0 at $\hat{\varepsilon}=\varepsilon$. This is because $\hat{\varepsilon}=\varepsilon$ is actually an extremum of the cost function based on the knowledge of calculus. Consequently, we have

$$J'(0)=2\pi B=0 \;\Rightarrow\; B=0. \tag{13}$$

With the results of Eqs. (12) and (13), Eq. (11) can be simplified as

$$J(\tilde{\varepsilon})=A\cos(2\pi\tilde{\varepsilon})-A, \quad A<0. \tag{14}$$

Eq. (14) shows that our cost function reaches its minimum value if and only if the CFO is truly compensated in the absence of noise. Thus, the identifiability problem is assured. We plot an example of the cost function in Fig. 1, where the actual CFO is 0.15. It is shown that our cost function is a sinusoidal curve and the precise estimate of CFO is in accordance with our expectation. Yao's and Zeng's methods are included here for comparison. Note that in Yao's method, the fourth-order statistics of kurtosis is minimized, while in Zeng's method, the power difference of data on each pair of neighboring subcarriers is minimized; thus, their cost functions can also be rearranged as the format of Eq. (11). However, the coefficient of the second term in Eq. (11) cannot be removed when a small number of OFDM symbols are used for Yao's method or the channel is frequency-selective for Zeng's method. This residual term would cause an inexact estimate of CFO (Zeng and Ghrayeb, 2008). However in our cost function, this undesired term can be ignored as long as the channel keeps constant during the estimation procedure.

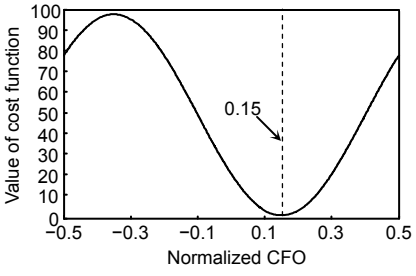

Fig. 1 An example of our cost function vs. normalized carrier frequency offset CFO in noise free case (N=32, CFO=0.15)

For real applications, there are always some VSCs embedded in OFDM symbols for various purposes. As proven in Appendix A, the proposed algorithm is still applicable with VSCs and the identifiability problem is also guaranteed. However, the estimation accuracy would degrade since the number of subcarriers able to be used for CFO estimation decreases.

3.3 Algorithm simplification

Minimizing the cost function can be done by exhaustive line search (Ma *et al*., 2001), but the complexity and estimation accuracy strictly depend on the grid that is used during the search (Gao and Nallanathan, 2006). Adaptive algorithms may also be applied but such parameters as the initial point and step size should be paid special attention to avoid failure (Talbot and Boroujeny, 2008), and the complexity is still high. Since our cost function is essentially a sinusoidal curve over the concerned estimation range, curve fitting can be utilized to simplify our algorithm (Yao and Giannakis, 2005). In real applications, A is not equal to $-C$ and furthermore B is not exactly 0 because of the presence of noise. Since B is still small enough, it is ignored. This approximation is reasonable as the numerical results show that our estimator using curve fitting achieves almost the optimal BER performance over different multipath channels. Accordingly, our cost function with noise is given by

$$J(\tilde{\varepsilon}) = A\cos(2\pi\tilde{\varepsilon}) + C. \tag{15}$$

We first calculate the value of Eq. (15) at several points before giving an estimate of the CFO, i.e.,

$$\begin{cases} J(\varepsilon - 0) = A\cos(2\pi\varepsilon) + C, \\ J(\varepsilon - 0.25) = A\cos 2\pi(\varepsilon - 0.25) + C = A\sin(2\pi\varepsilon) + C, \\ J(\varepsilon + 0.25) = A\cos 2\pi(\varepsilon + 0.25) + C = -A\sin(2\pi\varepsilon) + C. \end{cases} \tag{16}$$

Consequently, constants C and A can be calculated by

$$\begin{cases} C = [J(\varepsilon - 0.25) + J(\varepsilon + 0.25)]/2, \\ A = -[(J(\varepsilon) - C)^2 + (J(\varepsilon - 0.25) - C)^2]^{1/2}. \end{cases} \tag{17}$$

With Eqs. (16) and (17), it is easily demonstrated that

$$\hat{\varepsilon} = \begin{cases} +\arcsin(0.5 - (J(\varepsilon) - C)/2A)^{1/2}/\pi, \\ \qquad \text{if } \big(J(\varepsilon - 0.25) - C\big)/A > 0, \\ -\arcsin(0.5 - (J(\varepsilon) - C)/2A)^{1/2}/\pi, \\ \qquad \text{if } \big(J(\varepsilon - 0.25) - C\big)/A < 0. \end{cases} \tag{18}$$

Using curve fitting, only several points need to be calculated before coming to the final result and the global minimum is also guaranteed; thus, our algorithm has low complexity.

3.4 Performance analysis

In this part, we analytically assess the performance of the proposed estimator over the multipath channel in the presence of noise. The Cramér-Rao lower bound is not included in this study because of its equality to infinity without VSCs (Ghogho *et al*., 2001). In Meyrs and Franks (1980), by assuming at high SNR values, the expectation and mean square error (MSE) of our estimator can be well approximated by

$$E\{\hat{\varepsilon}\} \cong \varepsilon - \frac{E\{J'(\varepsilon)\}}{E\{J''(\varepsilon)\}},\ \mathrm{MSE}\{\hat{\varepsilon}\} \cong \frac{E\{[J'(\varepsilon)]^2\}}{[E\{J''(\varepsilon)\}]^2}, \tag{19}$$

where $J(\tilde{\varepsilon})$ is the cost function defined in Eq. (10), and $J'(\varepsilon)$ and $J''(\varepsilon)$ denote the first- and second-order derivatives of the cost function at $\hat{\varepsilon} = \varepsilon$, respectively. Supposing that the source symbol has unit energy, i.e., $\sigma_d^2 = 1$, we have Eq. (20):

$$\begin{aligned} &E\{\hat{\varepsilon}\} \cong \varepsilon, \\ &\mathrm{MSE}\{\hat{\varepsilon}\} \cong \\ &\frac{\sigma_n^2 \sum_{k=0}^{N-1} \left\{ \frac{N^4}{9} |H_k|^6 + \frac{7N^2}{3} \sum_{k \neq k'} \sin^2 \frac{(k-k')\pi}{N} |H_k|^4 |H_{k'}|^2 \right\}}{6\pi^2 \sigma_d^2 \left\{ \sum_{k=0}^{N-1} \sum_{k' \neq k} \frac{|H_k H_{k'}|^2}{\sin^2 \frac{(k-k')\pi}{N}} \right\}^2}. \end{aligned} \tag{20}$$

The proof of Eq. (20) is given in Appendix B.

The expectation ε reveals that our estimator is asymptotically unbiased. The analytical MSE depends on the OFDM block size N, the SNR, and the channel frequency response. To gain more insight into

Eq. (20), we suppose that the channel is frequency nonselective and N is sufficiently large; thus, the MSE can be well approximated as Eq. (21).

$$\mathrm{MSE}\{\hat{\varepsilon}\} \cong 4/(3\pi^2 \cdot \mathrm{SNR} \cdot N \cdot |H_k|^2). \tag{21}$$

Eq. (21) shows that the MSE of our estimator is inversely proportional to N and SNR. To verify the performance analysis, we compared the MSE obtained by numerical simulations with analytical results given by Eq. (20) in Fig. 2. A deterministic but unknown multipath channel (the channel model is CH1, which will be described in Section 5) is assumed and different block sizes are adopted. As shown in Fig. 2, the analytical results fit the numerical results well at medium-high SNR values and the MSE exhibits no error floor, which means the performance, improves as long as SNR increases.

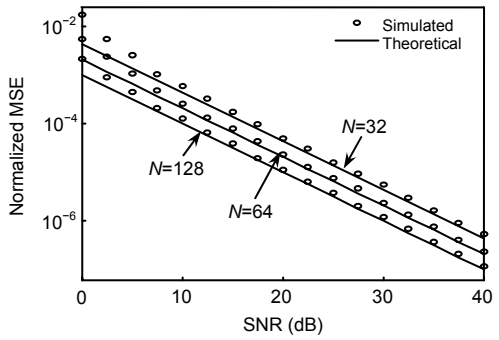

Fig. 2 MSE performance comparison between theoretical and numerical results with different values of the OFDM block size, *N*

4 Proposed CFO estimation scheme for MIMO-OFDM systems

In this section, we apply the proposed CFO estimator to a MIMO-OFDM system with M_T transmit antennas and M_R receive antennas. The channel frequency response between different transmit-receive antenna pairs is independent and identically distributed (i.i.d.). Also, different receive antennas experience a single common CFO (Yao and Giannakis, 2005). If there is perfect timing synchronization, the signal received by the rth receive antenna in the time domain can be

$$z_r(m) = \mathrm{e}^{\frac{\mathrm{j}2\pi\varepsilon[(m-1)N+mL]}{N}} \sum_{t=1}^{M_\mathrm{T}} \boldsymbol{\Phi}(\varepsilon)\boldsymbol{W}\boldsymbol{H}_{t,r}\boldsymbol{d}_t(m) + \boldsymbol{w}_r(m),$$
$$r = 1, 2, ..., M_\mathrm{R}, \tag{22}$$

where

$$\begin{cases} \boldsymbol{d}_t(m) = [d_{t,m,0}, d_{t,m,1}, ..., d_{t,m,N-1}]^\mathrm{T}, \\ \boldsymbol{H}_{t,r} = \mathrm{diag}\{H_{t,r,m,0}, H_{t,r,m,1}, ..., H_{t,r,m,N-1}\}. \end{cases} \tag{23}$$

$\boldsymbol{d}_t$(m) and $\boldsymbol{H}_{t,r}$ denote the data transmitted from the tth transmit antenna and the channel frequency response between the tth transmit antenna and the rth receive antenna, respectively. As can be observed from Eq. (22), the signal received by each receive antenna is essentially a combination of the signal transmitted from all transmit antennas. In the receiver, the CFO is first estimated and then compensated as in the case of SISO-OFDM systems. Therefore, the output after CFO compensation in the frequency domain is given by

$$\boldsymbol{y}_r(m) = \boldsymbol{W}^\mathrm{H}\boldsymbol{\Phi}(-\hat{\varepsilon})\boldsymbol{z}_r(m)$$
$$= \mathrm{e}^{\mathrm{j}2\pi\varepsilon[(m-1)N+mL]/N} \sum_{t=1}^{M_\mathrm{T}} \boldsymbol{W}^\mathrm{H}\boldsymbol{\Phi}(\varepsilon-\hat{\varepsilon})\boldsymbol{W}\boldsymbol{H}_{t,r}\boldsymbol{d}_t(m) + \boldsymbol{v}_r(m),$$
$$r = 1, 2, ..., M_\mathrm{R}. \tag{24}$$

If the CFO can be exactly compensated, Eq. (24) reduces to

$$\boldsymbol{y}_r(m) = \sum_{t=1}^{M_\mathrm{T}} \boldsymbol{H}_{t,r}\boldsymbol{d}_t(m) + \boldsymbol{v}_r(m), \ r = 1, 2, ..., M_\mathrm{R},$$
$$\Rightarrow\ y_{r,m,n} = \sum_{t=1}^{M_\mathrm{T}} H_{t,r,m,n}d_{t,m,n} + v_{r,m,n}, \tag{25}$$

where $H_{t,r,m,n}$ denotes the channel frequency response on the nth subcarrier from the tth transmit antenna to the rth receive antenna. Unlike in SISO-OFDM systems, the amplitude of channel frequency response cannot be simply decoupled from the output by square amplitude operations when $\hat{\varepsilon} = \varepsilon$.

Space-time block codes (STBC) are usually used to improve the rate and error performance in MIMO systems (Stüber *et al*., 2004). With the application of Alamouti (1998)'s STBC, the amplitude of $H_{t,r,m,n}$ can be computed with the observation of two consecutive OFDM symbols (Zeng and Ghrayeb, 2007). Without loss of generality, we consider a MIMO-OFDM

system with two transmit antennas, while the situation with an arbitrary number of transmit antennas can be obtained using the same approach. Let the data be transmitted from two antennas on the nth subcarrier at the mth to (m+3)th OFDM symbol durations (Alamouti, 1998):

$$\begin{bmatrix} d_{1,m,n} & -d^*_{2,m,n} & d_{1,m+1,n} & -d^*_{2,m+1,n} \\ d_{2,m,n} & d^*_{1,m,n} & d_{2,m+1,n} & d^*_{1,m+1,n} \end{bmatrix}. \tag{26}$$

We assume that the channel keeps constant over four OFDM symbol durations. Therefore, if there is a perfect CFO correction, the corresponding DFT output on the nth subcarrier of the rth receive antenna over four OFDM symbol durations can be written as

$$\begin{cases} y_{r,m,n} = H_{1,r,m,n} d_{1,m,n} + H_{2,r,m,n} d_{2,m,n}, \\ y_{r,m+1,n} = -H_{1,r,m,n} d^*_{2,m,n} + H_{2,r,m,n} d^*_{1,m,n}, \\ y_{r,m+2,n} = H_{1,r,m,n} d_{1,m+1,n} + H_{2,r,m,n} d_{2,m+1,n}, \\ y_{r,m+3,n} = -H_{1,r,m,n} d^*_{2,m+1,n} + H_{2,r,m,n} d^*_{1,m+1,n}. \end{cases} \tag{27}$$

Here we omit the noise term for brevity. Applying the square amplitude operation on Eq. (27), we can obtain

$$\begin{cases} \left|y_{r,m,n}\right|^2 = \left|H_{1,r,m,n}\right|^2 + \left|H_{2,r,m,n}\right|^2 \\ \quad + H_{1,r,m,n} d_{1,m,n} H^*_{2,r,m,n} d^*_{2,m,n} + H^*_{1,r,m,n} d^*_{1,m,n} H_{2,r,m,n} d_{2,m,n}, \\ \left|y_{r,m+1,n}\right|^2 = \left|H_{1,r,m,n}\right|^2 + \left|H_{2,r,m,n}\right|^2 \\ \quad - H_{1,r,m,n} d_{1,m,n} H^*_{2,r,m,n} d^*_{2,m,n} - H^*_{1,r,m,n} d^*_{1,m,n} H_{2,r,m,n} d_{2,m,n}, \\ \left|y_{r,m+2,n}\right|^2 = \left|H_{1,r,m,n}\right|^2 + \left|H_{2,r,m,n}\right|^2 \\ \quad + H_{1,r,m,n} d_{1,m+1,n} H^*_{2,r,m,n} d^*_{2,m+1,n} \\ \quad + H^*_{1,r,m,n} d^*_{1,m+1,n} H_{2,r,m,n} d_{2,m+1,n}, \\ \left|y_{r,m+3,n}\right|^2 = \left|H_{1,r,m,n}\right|^2 + \left|H_{2,r,m,n}\right|^2 \\ \quad - H_{1,r,m,n} d_{1,m+1,n} H^*_{2,r,m,n} d^*_{2,m+1,n} \\ \quad - H^*_{1,r,m,n} d^*_{1,m+1,n} H_{2,r,m,n} d_{2,m+1,n}. \end{cases} \tag{28}$$

Interestingly, the undesired terms in Eq. (28) can be simply removed according to Zeng and Ghrayeb (2007), as shown in Eq. (29):

$$\begin{cases} \left|y_{r,m,n}\right|^2 + \left|y_{r,m+1,n}\right|^2 = 2\left|H_{1,r,m,n}\right|^2 + 2\left|H_{2,r,m,n}\right|^2, \\ \left|y_{r,m+2,n}\right|^2 + \left|y_{r,m+3,n}\right|^2 = 2\left|H_{1,r,m,n}\right|^2 + 2\left|H_{2,r,m,n}\right|^2. \end{cases} \tag{29}$$

Based on the observation of Eqs. (28) and (29), the cost function of our estimator in the MIMO-OFDM system is shown in Eq. (30):

$$J(\tilde{\varepsilon}) = \sum_{r=1}^{M_r} \sum_{n=0}^{N-1} \left(\left|y_{r,m,n}\right|^2 + \left|y_{r,m+1,n}\right|^2 - \left|y_{r,m+2,n}\right|^2 - \left|y_{r,m+3,n}\right|^2 \right)^2. \tag{30}$$

Once again, our estimator needs more OFDM symbols than Zeng's and Yao's methods since ours takes advantage of the invariance of channel in the time domain whereas the other two exploit the invariance in the frequency domain. One can verify the identifiability problem in the same way as in the SISO-OFDM case and curve fitting can also be applied to simplify the minimization procedure of Eq. (30).

5 Numerical results

Numerical simulations have been conducted to show the efficiency of the proposed scheme. The simulation results are compared with those of Zeng's and Yao's methods in terms of MSE and BER.

5.1 Simulation parameters

The considered OFDM system has a block length of N=32 and a CP length of 8. The carrier frequency is 2.4 GHz, and the available bandwidth is 5 MHz. In our simulation, transmitted source symbols are modulated by quadrature phase-shift keying (QPSK). The normalized CFO is uniformly distributed in the range (−0.5, 0.5]. All results are averaged over 10 000 independent Monte Carlo simulations. The multipath channel is an exponentially decayed Rayleigh fading channel and the channel impulse response (CIR) is given by (O'Hara and Petrick, 1999)

$$\begin{cases} h_k = \mathcal{N}(0, \sigma_k^2/2) + \mathrm{j}\mathcal{N}(0, \sigma_k^2/2), \\ \sigma_k^2 = \sigma_0^2 \exp(-kT_S / T_{RMS}),\ \sigma_0^2 = 1 - \exp(T_S / T_{RMS}), \end{cases} \tag{31}$$

where $\mathcal{N}(0, \sigma_k^2/2)$ represents the Gaussian random

variable with zero mean and variance $\sigma_k^2/2$; T_S is the baseband sample rate, which is 0.2 μs in this study; T_{RMS} is the root mean squared delay spread, which is an environmental parameter. Three channels with T_{RMS} of 222, 404 and 528 ns are exploited in simulations, which will be referred to as CH1, CH2 and CH3 respectively. The maximum length of the channel is given by $10 \cdot T_{RMS}/T_S$. For each realization, the channel is randomly generated and kept constant during estimation.

5.2 SISO-OFDM systems

Fig. 3 demonstrates the MSE of the proposed algorithm with different numbers of VSCs over CH1. It is shown that the fully loaded system has the best performance since all subcarriers can be utilized for CFO estimation and there is only a slight degradation with up to 12 VSCs. Therefore, we assume that all the subcarriers are used for data carrying in the following simulations, just as in (Yao and Giannakis, 2005; Roman *et al*., 2006; Zeng and Ghrayeb, 2008).

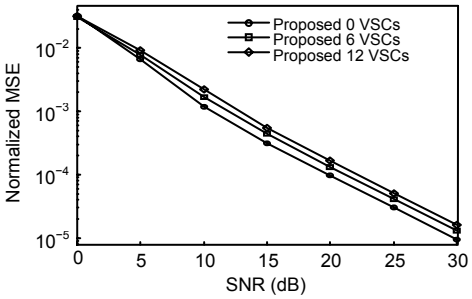

Fig. 3 MSE performance of the proposed estimator with different numbers of VSCs in SISO-OFDM systems

The proposed algorithm is compared with Zeng's and Yao's methods since they both need no pilots or VSCs. Two consecutive OFDM symbols are exploited during estimation. Fig. 4a shows the normalized MSE of the candidate estimators versus SNR over three different fading channels. We observe from the figure that our estimator displays a distinct superiority over the others, especially when SNR is high. Interestingly, Zeng's method performs better than our proposed estimator at low SNR values under CH1. However, both Zeng's and Yao's methods exhibit an error floor over three channels. This phenomenon can be attributed to the fact that both of these methods have internal interference, introduced by the channel's frequency selectivity, with constant energy over specific channels. The dominant factor associated with MSE performance is the additive noise; it can be referred to the external interference, when SNR is low, whereas the internal interference dominates as SNR augments. Since the channel's frequency selectivity increases accordingly from CH1 to CH3, the error floor takes place earlier in the SNR coordinate (Fig. 4a).

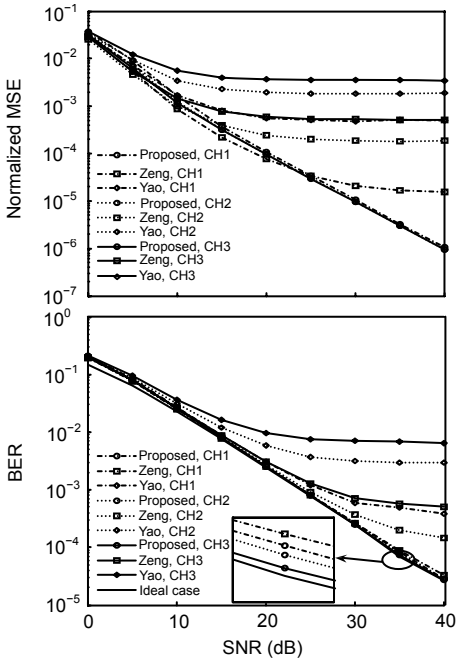

Fig. 4 (a) MSE and (b) BER performance of different CFO estimators over three channels in SISO-OFDM systems where two consecutive OFDM symbols are used

Fig. 4b compares the BER performance among different estimators over three fading channels. We assume the receiver has a perfect knowledge of the channel frequency response. Also, the BER obtained with true CFO compensation is included as the benchmark. It is observed that our estimator performs the best among the three estimators and almost achieves the optimal BER performance compared with the benchmark, only showing slight degradation when SNR is lower than 10 dB. In addition, notice that the BER of our method keeps nearly identical in three cases, which reveals the robustness to the channel's frequency selectivity. For Yao's method, the error floor in the CFO estimation results in another

error floor in the BER curve. On the other hand, although Zeng's method exhibits an error floor in the MSE over CH1, this floor does not translate into an error floor in BER; in fact, it has roughly the same performance as our method in this instance.

Fig. 5 illustrates the MSE and BER performance of the three CFO estimators when 10 consecutive OFDM symbols are applied, respectively. The performance of both Zeng's and Yao's methods improves, in accordance with the results in (Yao and Giannakis, 2005; Zeng and Ghrayeb, 2008). For the proposed algorithm, only the MSE continues to decrease, but showing no further improvement in BER. This is because our estimator already obtains nearly the optimal BER performance using two OFDM symbols.

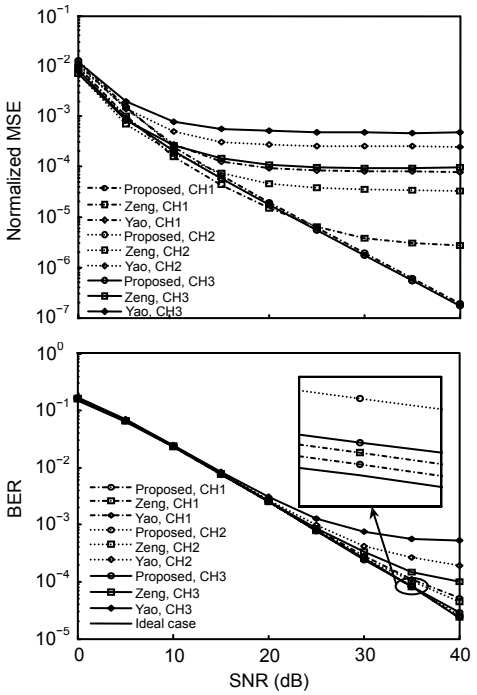

Fig. 5 (a) MSE and (b) BER performance of different CFO estimators over three channels in SISO-OFDM systems where ten consecutive OFDM symbols are used

5.3 MIMO-OFDM systems

The simulated MIMO-OFDM system has two transmit antennas and one receive antenna. Simulations are accomplished within four consecutive OFDM symbols. The MSE and BER of different estimators are shown in Figs. 6a and 6b, respectively. In Fig. 6a, our estimator exhibits performance improvements compared with the results in Fig. 4a since more symbols are utilized during estimation. Different from the SISO-OFDM case, our estimator has the best performance over the whole SNR range. As before, both Yao's and Zeng's methods have an error floor and our proposed estimator behaves nearly the same over three multipath channels. The BER performance of our estimator improves a lot because of the application of the Alamouti's STBC. Once again, our method achieves almost the optimal BER performance except for little degradation at SNR values lower than 10 dB. Zeng's method performs as well as our estimator under CH1 because the impact of the frequency selectivity is minor in this situation, whereas both Yao's and Zeng's methods display an error floor over CH2 and CH3 in BER curves.

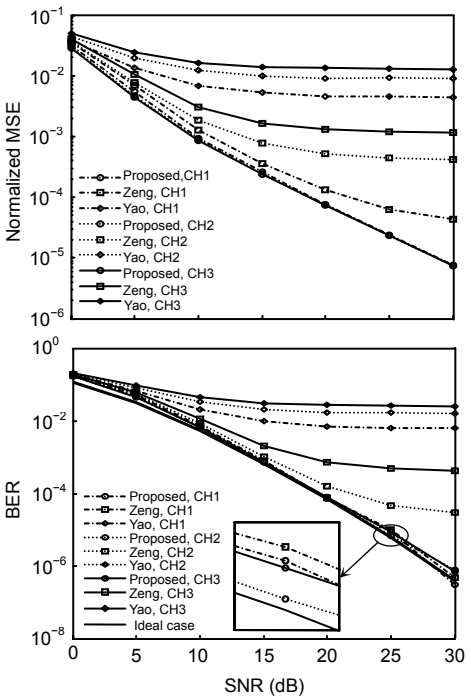

Fig. 6 (a) MSE and (b) BER performance of different CFO estimators over three channels in MIMO-OFDM systems where four consecutive OFDM symbols are used

6 Conclusion

In this paper, we proposed a blind CFO estimator for both SISO- and MIMO-OFDM systems with CM signaling. This algorithm is based on a reasonable assumption that the channel fading is slow enough so that the channel keeps constant while the CFO

estimation is performed. We proved the identifiability problem of our blind method. The sinusoid-like cost function enlightened us to exploit curve fitting to derive a low-complexity algorithm. Performance analysis showed that our estimator is asymptotically unbiased and the MSE performance depends on several factors, including the block size N, the SNR and the channel frequency response. Numerical results revealed that our estimator is robust to the channel's frequency selectivity and obtains almost the optimal BER performance in both SISO- and MIMO-OFDM systems.

Since pilots and VSCs are often embedded in OFDM symbols for channel estimation and synchronization or preserved for future use, further studies may focus on how to combine pilots and VSCs with the CM signaling to design an algorithm with an enlarged estimation range.

References

Ai, B., Yang, Z.X., Pan, C.Y., Ge, J.H., Wang, Y., Lu, Z., 2006. On the synchronization techniques for wireless OFDM systems. *IEEE Trans. Broadcast.*, **52**(2):236-244. [doi:10.1109/TBC.2006.872990]

Alamouti, S.M., 1998. A simple transmit diversity technique for wireless communications. *IEEE J. Sel. Areas Commun.*, **16**(8):1451-1458. [doi:10.1109/49.730453]

Coulson, A.J., 2001. Maximum likelihood synchronization for OFDM using a pilot symbol: algorithms. *IEEE J. Sel. Areas Commun.*, **19**(12):2486-2494. [doi:10.1109/49.974613]

Gao, F., Nallanathan, A., 2006. Blind maximum likelihood CFO estimation for OFDM systems via polynomial rooting. *IEEE Signal Process. Lett.*, **13**(2):73-76. [doi:10.1109/LSP.2005.861583]

Gao, F., Cui, T., Nallanathan, A., 2008. Scattered pilots and virtual carriers based frequency offset tracking for OFDM systems: algorithms, identifiability, and performance analysis. *IEEE Trans. Commun.*, **56**(4):619-629. [doi:10.1109/TCOMM.2008.060050]

Ghogho, M., Swami, A., Giannakis, G.B., 2001. Optimized Null-Subcarrier Selection for CFO Estimation in OFDM Over Frequency-Selective Fading Channels. IEEE GLOBECOM, **1**:202-206.

Hsieh, M.H., Wei, C.H., 1999. A low-complexity frame synchronization and frequency offset compensation scheme for OFDM systems over fading channels. *IEEE Trans. Veh. Technol.*, **48**(5):1596-1609. [doi:10.1109/25.790537]

Huang, D., Letaief, K.B., 2006. Carrier frequency offset estimation for OFDM systems using null subcarriers. *IEEE Trans. Commun.*, **54**(5):813-823. [doi:10.1109/TCOMM.2006.874001]

IEEE Std. 802.11a, 1999. Wireless LAN Medium Access Control (MAC) and Physical Layer (PHY) Specifications: High Speed Physical Layer in the 5 GHz Band. IEEE, Piscataway, NJ 08854-1331.

IEEE Std. 802.16, 2004. IEEE Standard for Local and Metropolitan Area Networks, Part 16: Air Interface for Fixed Broadband Wireless Access Systems. IEEE, Piscataway. NJ 08854-1331.

Lashkarian, N., Kiaei, S., 2000. Class of cyclic-based estimators for frequency-offset estimation of OFDM systems. *IEEE Trans. Commun.*, **48**(12):2139-2149. [doi:10.1109/26.891224]

Liu, H., Tureli, U., 1998. A high-efficiency carrier estimator for OFDM communications. *IEEE Commun. Lett.*, **2**(4):104-106. [doi:10.1109/4234.664219]

Lv, T., Li, H., Chen, J., 2005. Joint estimation of symbol timing and carrier frequency offset of OFDM signal over fast time-varying multipath channels. *IEEE Trans. Signal Process.*, **53**(12):4526-4535. [doi:10.1109/TSP.2005.859233]

Ma, X., Tepedelenlioglu, C., Giannakis, G.B., Barbarossa S., 2001. Nondata-aided carrier offset estimators for OFDM with null subcarriers: identifiability, algorithms, and performance. *IEEE J. Sel. Areas Commun.*, **19**(12):2504-2515. [doi:10.1109/49.974615]

Meyrs, M.H., Franks, L., 1980. Joint carrier phase and symbol timing recovery for PAM systems. *IEEE Trans. Commun.*, **28**(8):1121-1129. [doi:10.1109/TCOM.1980.1094811]

Minn, H., Bhargava, V.K., Letaief, K.B., 2003. A robust timing and frequency synchronization for OFDM systems. *IEEE Trans. Wirel. Commun.*, **2**(4):822-839. [doi:10.1109/TWC.2003.814346]

Minn, H., Bhargava, V.K., Letaief, K.B., 2006. A combined timing and frequency synchronization and channel estimation for OFDM. *IEEE Trans. Commun.*, **54**(3):416-422. [doi:10.1109/TCOMM.2006.869860]

Moose, P.H., 1994. A technique for orthogonal frequency division multiplexing frequency offset correction. *IEEE Trans. Commun.*, **42**(10):2908-2914. [doi:10.1109/26.328961]

Morelli, M., D′Andrea, A.N., Mengali, U., 2000. Frequency ambiguity resolution in OFDM systems. *IEEE Commun. Lett.*, **4**(4):134-136. [doi:10.1109/4234.841321]

Morelli, M., Kuo, C.C.J., Pun, M.O., 2007. Synchronization techniques for orthogonal frequency division multiple access (OFDMA): a tutorial review. *Proc. IEEE*, **95**(7):1394-1427. [doi:10.1109/JPROC.2007.897979]

O′Hara, B., Petrick, A., 1999. The IEEE 802.11 Handbook: A Designer's Companion. The Institute of Electrical and Electronics Engineers, Inc.

Pollet, T., van Bladel, M., Moeneclaey, M., 1995. BER sensitivity of OFDM systems to carrier frequency offset and Wiener phase noise. *IEEE Trans. Commun.*, **43**(2):191-193. [doi:10.1109/26.380034]

Roman, T., Visuri, S., Koivunen, V., 2006. Blind frequency

synchronization in OFDM via diagonality criterion. *IEEE Trans. Signal Process.*, **54**(8):3125-3135. [doi:10.1109/TSP.2006.877636]

Schmidl, T.M., Cox, D.C., 1997. Robust frequency and timing synchronization for OFDM. *IEEE Trans. Commun.*, **45**(12):1613-1621. [doi:10.1109/26.650240]

Stüber, G.L., Barry, J.R., McLaughlin, S.W., Li, Y., Ingram, M.A., Pratt, T.G., 2004. Broadband MIMO-OFDM wireless communications. *Proc. IEEE*, **92**(2):271-294. [doi:10.1109/JPROC.2003.821912]

Talbot, S.L., Boroujeny, B.F., 2008. Spectral method of blind carrier tracking for OFDM. *IEEE Trans. Signal Process.*, **56**(7):2706-2717. [doi:10.1109/TSP.2008.917377]

Tureli, U., Liu, H., Zoltowski, M.D., 2000. OFDM blind carrier offset estimation: ESPRIT. *IEEE Trans. Commun.*, **48**(9):1459-1461. [doi:10.1109/26.870011]

Tureli, U., Kivanc, D., Liu, H., 2001. Experimental and analytical studies on a high-resolution OFDM carrier frequency offset estimator. *IEEE Trans. Veh. Technol.*, **50**(2):629-643. [doi:10.1109/25.923074]

Tureli, U., Honan, P.J., Liu, H., 2004. Low-complexity nonlinear least squares carrier offset estimator for OFDM: identifiability, diversity and performance. *IEEE Trans. Signal Process.*, **52**(9):2441-2452. [doi:10.1109/TSP.2004.831918]

van de Beek, J.J., van de Sandell, M., Börjesson, P.O., 1997. ML estimation of time and frequency offset in OFDM systems. *IEEE Trans. Signal Process.*, **45**(7):1800-1805. [doi:10.1109/78.599949]

van Nee, R., Prasad, R., 2000. OFDM for Wireless Multimedia Communications. Artech House, London, p.33-48.

Yao, Y., Giannakis, G.B., 2005. Blind carrier frequency offset estimation in SISO, MIMO, and multiuser OFDM systems. *IEEE Trans. Commun.*, **53**(1):173-183. [doi:10.1109/TCOMM.2004.840623]

Yu, J.H., Su, Y.T., 2004. Pilot-assisted maximum-likelihood frequency-offset estimation for OFDM systems. *IEEE Trans. Commun.*, **52**(11):1997-2008. [doi:10.1109/TCOMM.2004.836555]

Zeng, X.N., Ghrayeb, A., 2007. A Blind Carrier Frequency Offset Estimation Scheme for OFDM Systems with Constant Modulus Signaling. IEEE Workshop on Signal Processing Advances in Wireless Communications, p.1-5.

Zeng, X.N., Ghrayeb, A., 2008. A blind carrier frequency offset estimation scheme for OFDM systems with constant modulus signaling. *IEEE Trans. Commun.*, **56**(7):1032-1037. [doi:10.1109/TCOMM.2008.060585]

Appendix A: Derivation of Eq. (11)

In the presence of a CFO ε, the DFT output on the nth subcarrier of the mth symbol can be written as

$$y_{m,n}(\tilde{\varepsilon})=\frac{1}{N}\sum_{k=0}^{N-1}d_{m,k}H_k\sum_{p=0}^{N-1}\mathrm{e}^{\mathrm{j}2\pi(\tilde{\varepsilon}+k-n)p/N}. \quad \text{(A1)}$$

We use H_k to denote $H_{m,k}$ and $H_{m+1,k}$ since the channel frequency response remains the same over two consecutive OFDM symbols. Then we could have

$$\begin{aligned}\sum_{n=0}^{N-1}\left|y_{m,n}(\tilde{\varepsilon})\right|^4=&\frac{1}{N^4}\sum_{n=0}^{N-1}\sum_{k_1,k_2,k_3,k_4=0}^{N-1}\tilde{y}_{m,k_1}\tilde{y}_{m,k_2}^{*}\tilde{y}_{m,k_3}\tilde{y}_{m,k_4}^{*}\\&\cdot\sum_{p_1,p_2,p_3,p_4=0}^{N-1}\left\{\mathrm{e}^{\mathrm{j}2\pi[p_1k_1-p_2k_2+p_3k_3-p_4k_4+(p_1-p_2+p_3-p_4)\tilde{\varepsilon}]}\right.\\&\left.\cdot\mathrm{e}^{-\mathrm{j}2\pi(p_1-p_2+p_3-p_4)n/N}\right\},\end{aligned} \quad \text{(A2)}$$

where $\tilde{y}_{m,k}=d_{m,k}H_k$. It is observed that the summands of Eq. (A2) are not equal to 0 only under several conditions, namely, when $p_1-p_2+p_3-p_4=0, \pm N$. As a consequence, Eq. (A2) can be expanded as Eq. (A3):

$$\begin{aligned}\sum_{n=0}^{N-1}\left|y_{m,n}(\tilde{\varepsilon})\right|^4=&\frac{1}{N^3}\sum_{k_1,k_2,k_3,k_4=0}^{N-1}\tilde{y}_{m,k_1}\tilde{y}_{m,k_2}^{*}\tilde{y}_{m,k_3}\tilde{y}_{m,k_4}^{*}\\&\cdot\left(\mathrm{e}^{-\mathrm{j}2\pi\tilde{\varepsilon}}\sum_{\substack{p_1,p_2,p_3,p_4=0\\p_1-p_2+p_3-p_4=-N}}^{N-1}\mathrm{e}^{\mathrm{j}2\pi(p_1k_1-p_2k_2+p_3k_3-p_4k_4)/N}\right.\\&+\mathrm{e}^{\mathrm{j}2\pi\tilde{\varepsilon}}\sum_{\substack{p_1,p_2,p_3,p_4=0\\p_1-p_2+p_3-p_4=N}}^{N-1}\mathrm{e}^{\mathrm{j}2\pi(p_1k_1-p_2k_2+p_3k_3-p_4k_4)/N}\\&\left.+\sum_{\substack{p_1,p_2,p_3,p_4=0\\p_1-p_2+p_3-p_4=0}}^{N-1}\mathrm{e}^{\mathrm{j}2\pi(p_1k_1-p_2k_2+p_3k_3-p_4k_4)/N}\right).\end{aligned} \quad \text{(A3)}$$

After some algebraic manipulations, we find the first two terms of Eq. (A3) are a conjugate pair and the last term is a real constant. Therefore, Eq. (A3) can be rewritten in a more compact form as shown in

$$\sum_{n=0}^{N-1}\left|y_{m,n}(\tilde{\varepsilon})\right|^4=A_1\cos(2\pi\tilde{\varepsilon})+B_1\sin(2\pi\tilde{\varepsilon})+C_1, \quad \text{(A4)}$$

where A_1, B_1 and C_1 are constants which depend only on data and channel realization. Using the same approach, the second and third terms in Eq. (10) would be rearranged as

$$\begin{cases} \sum_{n=0}^{N-1}\left|y_{m,n}(\tilde{\varepsilon})\right|^4 = A_2\cos(2\pi\tilde{\varepsilon}) + B_2\sin(2\pi\tilde{\varepsilon}) + C_2, \\ 2\sum_{n=0}^{N-1}\left(\left|y_{m,n}(\tilde{\varepsilon})\right|^2 \cdot \left|y_{m+1,n}(\tilde{\varepsilon})\right|^2\right) \\ \qquad = A_3\cos(2\pi\tilde{\varepsilon}) + B_3\sin(2\pi\tilde{\varepsilon}) + C_3. \end{cases} \tag{A5}$$

Summing Eqs. (A4) and (A5), we can obtain Eq. (11).

We then consider the applicability of the proposed algorithm in the presence of VSCs. Without loss of generality, it is assumed that the first N_u subcarriers are used for data carrying and the last $N-N_u$ subcarriers are VSCs. Hence, Eq. (A1) can be rewritten as

$$y_{m,n}(\tilde{\varepsilon}) = \frac{1}{N}\sum_{k=0}^{N_u-1} d_{m,k}H_k \sum_{p=0}^{N-1} \mathrm{e}^{\mathrm{j}2\pi(\tilde{\varepsilon}+k-n)p/N}. \tag{A6}$$

Note that k ranges from 0 to N_u-1 since not all subcarriers are used for data transmission, while p and n range from 0 to N because there are still N points IDFT and DFT output. Therefore, Eq. (A2) changes to

$$\begin{aligned} \sum_{n=0}^{N-1}\left|y_{m,n}(\tilde{\varepsilon})\right|^4 &= \frac{1}{N^4}\sum_{n=0}^{N-1}\sum_{k_1,k_2,k_3,k_4=0}^{N_u-1} \tilde{y}_{m,k_1}\tilde{y}^*_{m,k_2}\tilde{y}_{m,k_3}\tilde{y}^*_{m,k_4} \\ &\cdot \sum_{p_1,p_2,p_3,p_4=0}^{N-1} \left\{\mathrm{e}^{\mathrm{j}2\pi[p_1k_1-p_2k_2+p_3k_3-p_4k_4+(p_1-p_2+p_3-p_4)\tilde{\varepsilon}]} \right. \\ &\left. \cdot\, \mathrm{e}^{-\mathrm{j}2\pi(p_1-p_2+p_3-p_4)n/N}\right\}. \end{aligned} \tag{A7}$$

This equation can also be rearranged as the format of Eq. (A4). Hence the cost function of the proposed method is still a cosine wave over (−0.5, +0.5] in the presence of VSCs and the identifiability problem is assured.

Appendix B: Derivation of Eq. (20)

First, we denote the received data on the nth subcarrier of the mth symbol after DFT by the summation of source symbol and additive noise, i.e.,

$$y_{m,n} = \overline{y}_{m,n} + v_{m,n}, \tag{B1}$$

where $\overline{y}_{m,n}$ and $v_{m,n}$ are mutually independent. Here we drop the notation of '$(\tilde{\varepsilon})$' for derivation simplicity. Using Eq. (B1), the first term of Eq. (10) in the presence of noise can be expanded as

$$\begin{aligned} \sum_{n=0}^{N-1}\left|y_{m,n}\right|^4 = \sum_{n=0}^{N-1}\Big[&\left|\overline{y}_{m,n}\right|^4 + \left|v_{m,n}\right|^4 \\ &+4\left|\overline{y}_{m,n}\right|^2\left|v_{m,n}\right|^2 + (\overline{y}^*_{m,n}v_{m,n})^2 + (v^*_{m,n}\overline{y}_{m,n})^2 \\ &+4\left|\overline{y}_{m,n}\right|^2\Re\left\{\overline{y}^*_{m,n}v_{m,n}\right\} + 4\left|v_{m,n}\right|^2\Re\left\{\overline{y}^*_{m,n}v_{m,n}\right\}\Big]. \end{aligned} \tag{B2}$$

Applying the first-order approximation and assuming that the SNR value is sufficiently large, Eq. (B2) can be approximated as

$$\sum_{n=0}^{N-1}\left|y_{m,n}\right|^4 \cong \sum_{n=0}^{N-1}\left[\left|\overline{y}_{m,n}\right|^4 + 4\left|\overline{y}_{m,n}\right|^2\Re\left\{\overline{y}^*_{m,n}v_{m,n}\right\}\right]. \tag{B3}$$

The other two terms in Eq. (10) can be manipulated similarly. Thus, our cost function with noise can be rewritten as

$$\begin{aligned} J(\tilde{\varepsilon}) \cong \sum_{n=0}^{N-1}\Big[&\left|\overline{y}_{m,n}\right|^4 + \left|\overline{y}_{m+1,n}\right|^4 - 2\left|\overline{y}_{m,n}\right|^2\left|\overline{y}_{m+1,n}\right|^2 \\ &+4\left|\overline{y}_{m,n}\right|^2\Re\left\{\overline{y}^*_{m,n}v_{m,n}\right\} + 4\left|\overline{y}_{m+1,n}\right|^2\Re\left\{\overline{y}^*_{m+1,n}v_{m+1,n}\right\} \\ &-4\left|\overline{y}_{m+1,n}\right|^2\Re\left\{\overline{y}^*_{m,n}v_{m,n}\right\} - 4\left|\overline{y}_{m,n}\right|^2\Re\left\{\overline{y}^*_{m+1,n}v_{m+1,n}\right\}\Big]. \end{aligned} \tag{B4}$$

It is easily derived that the mean of the first order derivative of the cost function at $\hat{\varepsilon} = \varepsilon$ is 0 owing to the presence of the noise term, which demonstrates that our proposed estimator is asymptotically unbiased, i.e.,

$$E\{\hat{\varepsilon}\} \cong \varepsilon. \tag{B5}$$

For the MSE in Eq. (19), we first consider the denominator. The expectation of the second order derivative of our cost function can be given by

$$\begin{aligned} &E\{J''(\varepsilon)\} \\ &= E\left\{\sum_{n=0}^{N-1}\frac{\mathrm{d}^2\left(\left|\overline{y}_{m,n}\right|^4 + \left|\overline{y}_{m+1,n}\right|^4 - 2\left|\overline{y}_{m,n}\right|^2\left|\overline{y}_{m+1,n}\right|^2\right)}{\mathrm{d}\hat{\varepsilon}^2}\bigg|_{\hat{\varepsilon}=\varepsilon}\right\}, \end{aligned} \tag{B6}$$

while the other terms in Eq. (B4) have a zero mean because of the noise. We calculate the three terms in Eq. (B6) separately with the first term in the parentheses represented by

$$\sum_{n=0}^{N-1}\frac{\mathrm{d}^2\left|\overline{y}_{m,n}\right|^4}{\mathrm{d}\hat{\varepsilon}^2}\bigg|_{\hat{\varepsilon}=\varepsilon}$$
$$=\frac{-8\pi^2}{N^3}\Re\left\{\sum_{k_1,k_2,k_3,k_4=0}^{N-1}d_{m,k_1}d_{m,k_2}^{*}d_{m,k_3}d_{m,k_4}^{*}H_{k_1}H_{k_2}H_{k_3}H_{k_4}\right.$$
$$\left.\cdot\sum_{\substack{p_1,p_2,p_3,p_4=0\\ p_1-p_2+p_3-p_4=-N}}^{N-1}\mathrm{e}^{\mathrm{j}2\pi(p_1k_1-p_2k_2+p_3k_3-p_4k_4)/N}\right\}. \quad \text{(B7)}$$

We consider two different cases to calculate the expectation of Eq. (B7).

Case 1: $k_1=k_2=k_3=k_4$. The expectation of Eq. (B7) can be calculated as

$$T_1=\sum_{k=0}^{N-1}\left[\frac{-8\pi^2E\left\{\left|d_k^4\right|\right\}}{N^2}\times\frac{(N^2-1)\left|H_k\right|^4}{6}\right]. \quad \text{(B8)}$$

Case 2: $k_1=k_2\neq k_3=k_4$ or $k_1=k_4\neq k_3=k_2$. The expectation of Eq. (B7) can be calculated as

$$T_2=\sum_{k=0}^{N-1}\left[\frac{8\pi^2E\left\{\left|d_k^4\right|\right\}}{N^3}\times\sum_{k'\neq k}\frac{N\left|H_kH_{k'}\right|^2}{\sin^2\dfrac{(k-k')\pi}{N}}\right]. \quad \text{(B9)}$$

By adding T_1 and T_2, we can get the first term in Eq. (B6). It is observed that the second term is the same as the first one. When we come to the calculation of the third term, the only difference is in Case 2, which can be calculated as

$$T_2'=\sum_{k=0}^{N-1}\left[\frac{8\pi^2E\left\{\left|d_k^4\right|\right\}}{N^3}\times\sum_{k'\neq k}\frac{N\left|H_kH_{k'}\right|^2}{2\sin^2\dfrac{(k-k')\pi}{N}}\right]. \quad \text{(B10)}$$

With Eqs. (B8)–(B10), we can obtain the denominator.

It is more complex to calculate the numerator of the MSE in Eq. (19). First, we make the approximation

$$J'(\varepsilon)=\frac{\mathrm{d}}{\mathrm{d}\hat{\varepsilon}}\sum_{n=0}^{N-1}\Big[4\left|\overline{y}_{m,n}\right|^2\Re\left\{\overline{y}_{m,n}^{*}v_{m,n}\right\}$$
$$+4\left|\overline{y}_{m+1,n}\right|^2\Re\left\{\overline{y}_{m+1,n}^{*}v_{m+1,n}\right\} \quad \text{(B11)}$$
$$-4\left|\overline{y}_{m+1,n}\right|^2\Re\left\{\overline{y}_{m,n}^{*}v_{m,n}\right\}-4\left|\overline{y}_{m,n}\right|^2\Re\left\{\overline{y}_{m+1,n}^{*}v_{m+1,n}\right\}\Big]\Big|_{\hat{\varepsilon}=\varepsilon}.$$

Eq. (B11) is based on the fact that the first-order derivative of our cost function without noise is 0 at $\hat{\varepsilon}=\varepsilon$. Define the symbolic representation as

$$J'(\varepsilon)=\Psi_1+\Psi_2-\Psi_3-\Psi_4. \quad \text{(B12)}$$

The four symbols denote the corresponding terms in Eq. (B11). We find that the numerator could be calculated by

$$E\left\{\left[J'(\varepsilon)\right]^2\right\}=E\left\{(\Psi_1+\Psi_2-\Psi_3-\Psi_4)^2\right\}\cong\frac{4}{3}E\left\{\Psi_1^2\right\}, \quad \text{(B13)}$$

with Ψ_1 given by

$$\frac{\mathrm{d}}{\mathrm{d}\hat{\varepsilon}}\sum_{n=0}^{N-1}4\left|\overline{y}_{m,n}\right|^2\Re\left\{\overline{y}_{m,n}^{*}v_{m,n}\right\}\Big|_{\hat{\varepsilon}=\varepsilon}$$
$$=\frac{\mathrm{j}4\pi}{N^2\sqrt{N}}\sum_{\boldsymbol{k},\boldsymbol{p}}\tilde{y}_{m,k_1}\tilde{y}_{m,k_2}^{*}\mathrm{e}^{\mathrm{j}2\pi(p_ik_1-p_2k_2)/N} \quad \text{(B14)}$$
$$\cdot\left\{\tilde{y}_{m,k_3}v_{m,p_4}^{*}\mathrm{e}^{\mathrm{j}2\pi p_3k_3/N}[-1(\boldsymbol{p}\in\Omega^+)+1(\boldsymbol{p}\in\Omega^-)]\right.$$
$$\left.+\tilde{y}_{m,k_3}^{*}v_{m,p_4}\mathrm{e}^{-\mathrm{j}2\pi p_3k_3/N}[-1(\boldsymbol{p}\in\Theta^+)+1(\boldsymbol{p}\in\Theta^-)]\right\},$$

where $\boldsymbol{k}:=\{k_1, k_2, k_3, k_4\}$, $\boldsymbol{p}:=\{p_1, p_2, p_3, p_4\}$, 1() is the indicator function, and $\Omega^{\pm}$, $\Theta^{\pm}:=\{\boldsymbol{p}:|=p_1-p_2+p_3-p_4=\pm N\}$. Through some algebraic manipulations, we come to

$$E\left\{\left|\Psi_1\right|^2\right\}\cong\sum_{k=0}^{N-1}\left\{\frac{4\pi^2(N^2-1)^2}{9N^4}\left|H_k\right|^6E\left\{\left|d_k^6\right|\right\}\sigma_n^2\right.$$
$$\left.+\frac{28\pi^2(N^2-1)}{3N^4}\sum_{k\neq k'}\sin^2\frac{(k-k')\pi}{N}\left|H_k\right|^4\left|H_{k'}\right|^2E\left\{\left|d_k^6\right|\right\}\sigma_n^2\right\}. \quad \text{(B15)}$$

After substituting Eq. (B15) in Eq. (B13), we can obtain the numerator. With all the results above, Eq. (20) is verified.